doi:10.1016/j.jmb.2010.06.061 J. Mol. Biol. (2010) 401, 690–695

JMB

Available online at www.sciencedirect.com

ScienceDirect

ELSEVIER

COMMUNICATION

Glycosidic Bond Conformation Preference Plays a Pivotal Role in Catalysis of RNA Pseudouridylation: A Combined Simulation and Structural Study

Jing Zhou[1], Chao Lv[1], Bo Liang[2], Mengen Chen[2], Wei Yang[1,2]* and Hong Li[1,2]*

[1]*Department of Chemistry and Biochemistry, Florida State University, Tallahassee, FL 32306, USA*

[2]*Institute of Molecular Biophysics, Florida State University, Tallahassee, FL 32306, USA*

Received 5 May 2010; received in revised form 26 June 2010; accepted 29 June 2010
Available online 6 July 2010

Edited by D. Case

The most abundant chemical modification on RNA is isomerization of uridine (or pseudouridylation) catalyzed by pseudouridine synthases. The catalytic mechanism of this essential process remains largely speculative, partly due to lack of knowledge of the pre-reactive state that is important to the identification of reactive chemical moieties. In the present study, we showed, using orthogonal space random-walk free-energy simulation, that the pre-reactive states of uridine and its reactive derivative 5-fluorouridine, bound to a ribonucleoprotein particle pseudouridine synthase, strongly prefer the *syn* glycosidic bond conformation, while that of the nonreactive 5-bromouridine-containing substrate is largely populated in the *anti* conformation state. A high-resolution crystal structure of the 5-bromouridine-containing substrate bound to the ribonucleoprotein particle pseudouridine synthase and enzyme activity assay confirmed the *anti* nonreactive conformation and provided the molecular basis for its confinement. The observed preference for the *syn* pre-reactive state by the enzyme-bound uridine may help to distinguish among currently proposed mechanisms.

Keywords: pseudouridine synthase; H/ACA ribonucleoprotein; free energy simulation; catalytic mechanism; ring conformation

Despite its prevalence[1,2] and demonstrated importance in RNA structure[3–5] and function,[6,7] the catalytic mechanism of pseudouridylation remains largely speculative, partly due to lack of knowledge of the pre-reactive state critical to the identification of reactive chemical moieties. This process is thought to begin with the cleavage of the *N*-glycosyl bond (ring cleavage), followed by a 180° rotation of the uracil base while still enzyme bound (ring rotation), reattachment of the ring at C5 (ring reattachment), and, finally, deprotonation of C5[8–10] (Fig. 1). Cofactors are not known to be required for any of these steps.

In bacteria, approximately a dozen uridine residues in transfer RNA and ribosomal RNA (rRNA) are modified by six families of pseudouridine synthases: TruA, TruB, TruD, RluA, RsuA, and Pus10.[11–19] Each of these pseudouridine synthases is responsible for modifying one or several specific uridine nucleotides in transfer RNA or rRNA. In Archaea and Eukarya, where rRNA and small nuclear RNA are extensively modified, pseudouridylation is largely carried out by box H/ACA ribonucleoprotein particle (RNP) pseudouridine synthases.[20–24] Unlike stand-alone pseudouridine synthases, box H/ACA RNP pseudouridine synthases are multisubunit enzymes and comprise four protein subunits and one RNA subunit (Fig. 1a). The four protein subunits include Cbf5, Nop10, Gar1, and Nhp2 (L7Ae in Archaea). Cbf5 shares sequence motifs and a structural similarity with the TruB family of pseudouridine synthases and is the catalytic subunit of the RNP enzyme. The RNA

*Corresponding authors. W. Yang is to be contacted at Department of Chemistry and Biochemistry, Florida State University, Tallahassee, FL 32306, USA; H. Li, Department of Chemistry and Biochemistry, Florida State University, Tallahassee, FL 32306, USA. E-mail addresses: yyang2@fsu.edu; hong.li@fsu.edu.

Abbreviations used: rRNA, ribosomal RNA; RNP, ribonucleoprotein particle; 5FU, 5′-fluorouridine; 5FhΨ, 5-fluoro-6-hydroxpseudouridine; 5BrU, 5-bromouridine.

0022-2836/$ - see front matter. Published by Elsevier Ltd.

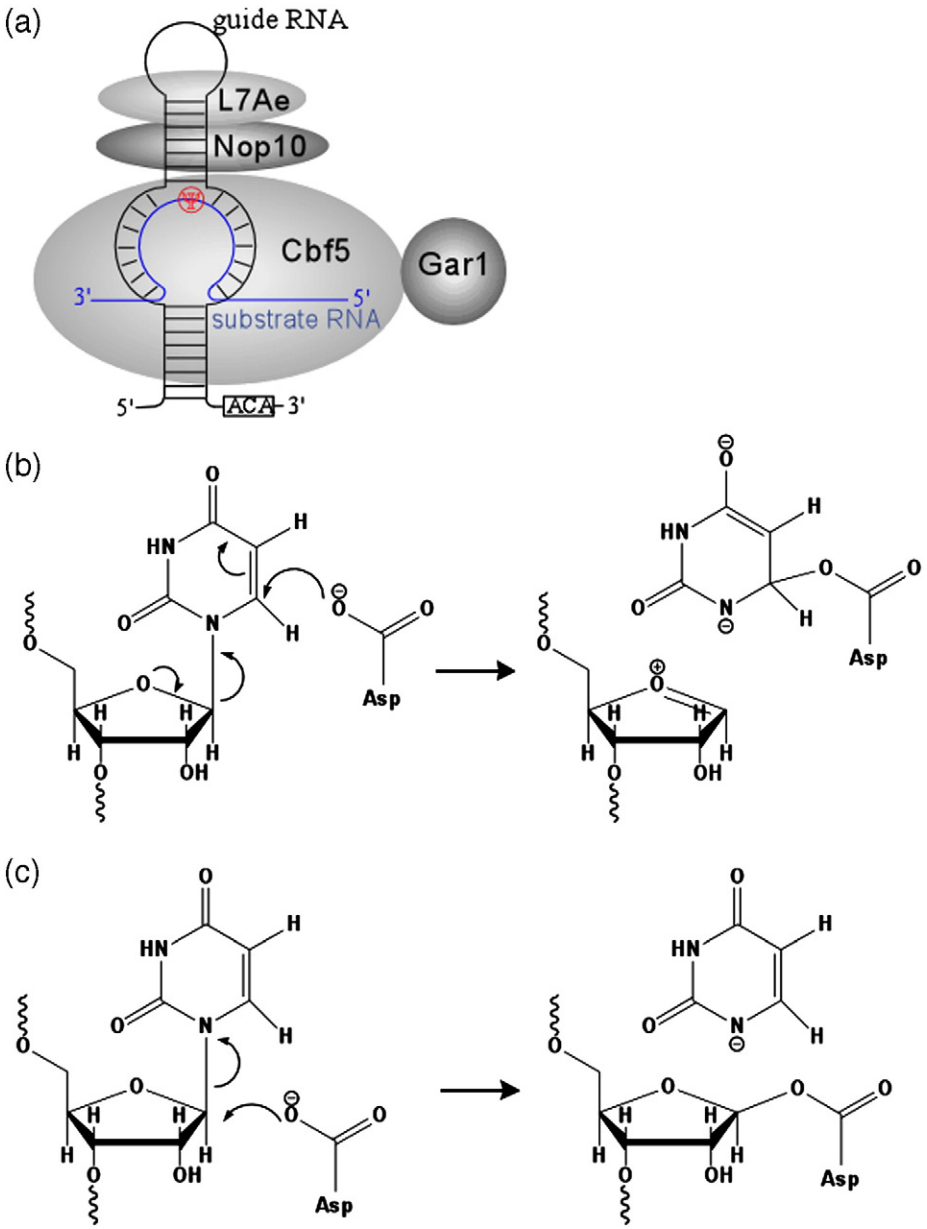

Fig. 1. Composition of the box H/ACA ribonucleoprotein particle pseudouridine synthase (a) and schematics of the two proposed mechanisms for pseudouridylation: Michael addition mechanism (b) and acylal mechanism (c). The two mechanisms share the same catalytic steps and the catalytic Asp residue but differ in the role that Asp plays in ring cleavage.

subunit belongs to the class of box H/ACA noncoding RNA and is characterized by a hairpin-like secondary structure and the strictly conserved ACA trinucleotide at its 3′ end.[20–24] Substrate RNA is captured by the RNP enzyme through its base-pairing with the central internal loop (pseudouridine pocket) of the box H/ACA RNA (Fig. 1a).

Regardless of their substrate specificity and enzyme composition, however, all families of pseudouridine synthases contain a well-conserved catalytic domain and a catalytic aspartate residue.[9,25,26] Mutation of catalytic Asp to Asn in bacterial TruB and TruA pseudouridine synthases resulted in complete loss of enzyme activity.[9,27] Furthermore, mutation of Asp to Ala in an archaeal H/ACA RNP also abolished modification activity,[28] suggesting that this residue is essential to catalysis.

Two mechanisms that invoke Asp as a nucleophile have been proposed for the catalytic process. In Michael addition mechanism (Fig. 1b), Asp attacks the RNA ring atom C6, leading to an Asp-Pyr covalent adduct. The strongest evidence supporting this mechanism is the observation on an RNA substrate containing 5′-fluorouridine (5FU) that *Escherichia coli* TruA and RluA either cross-link to or strongly interact with the hydrated product 5-fluoro-6-hydroxpseudouridine (5FhΨ).[29,30] In opposition to the proposed Michael addition mechanism, however, the crystal structures of TruB, RluA, and the H/ACA pseudouridine synthase bound to 5FU-substituted RNA substrates do not show a covalent intermediate, although it was argued in the case of the RluA–RNA complex that X-ray radiation used for diffraction studies dissolved the possible

covalent linkage.[17,19,31,32] Furthermore, the bound 5FhΨ in all cases has its C6 pointing away from the γ-carboxyl group of the catalytic Asp. The unfavorable ring orientation is also observed in the complex of the Asp-Asn TruB mutant bound to a 5FU-containing RNA substrate.[33] The second proposed mechanism is acylal mechanism (Fig. 1c), in which the catalytic Asp attacks the sugar atom C1′ to form the acylal intermediate that stabilizes the oxocarbonium ion. This mechanism should be less sensitive to the ring orientation than to the distance between Asp and C1′. Elucidation of the pseudouridine synthase mechanism thus requires an assessment of the glycosidic bond conformation of uridine in its pre-reactive state.

Previously, we obtained a cocrystal structure of a functional H/ACA RNP pseudouridine synthase bound to a guide RNA and a 5FU-containing substrate RNA.[32] This structure made it possible for us to explore the theoretical pre-reactive state of the substrate. We carried out free-energy simulation on the box H/ACA RNP complex containing the wild-type and 5FU substrates using the previously developed orthogonal space random-walk algorithm.[34,35] As detailed in Supplementary Data, we utilized a novel "alchemical" transition[36,37] scheme to realize the *syn*-to-*anti* conformation transformation about the glycosidic bond of uridine (Fig. 2a). The previously determined structure containing 5FhΨ was used to build the starting structures for the simulation by substituting 5FhΨ for uridine base. We found that for both the wild-type substrate and the 5FU-substituted substrate, the *syn* conformation is preferred to the *anti* conformation by −3.5 kcal/mol and −2.5 kcal/mol, respectively. This is in contrast to the *anti* conformation of 5-fluorouridine captured in the TruB D48N crystal structure containing 5FU,[33] suggesting that the D48N mutation may sufficiently disturb the microenvironment of the active site to favor the *anti* conformation.

The *syn* conformation places the ring C6 atom close to the catalytic Asp85 (Fig. 2b). In order to test the importance of the *syn* conformation to catalysis, we carried out the same free-energy simulation on a 5-bromouridine (5BrU)-containing substrate bound to H/ACA RNP. Bromine is less electronegative but bulkier in size than fluorine. Consistently, 5BrU was found to prefer the *anti* conformation to the *syn* conformation by more than 8 kcal/mol (Fig. 2b), suggesting that it may be defective in the ring cleavage step.

To determine if 5BrU is a substrate for the pseudouridine synthase, we used the DNA splint technique for constructing both wild-type substrate RNA and 5BrU-containing substrate RNA from two synthetic oligos[38] with a ^{32}P label on the 5′ position of the target uridine or modified uridine. The integrity of the ligated substrate RNA was checked on a denaturing polyacrylamide gel (data not shown). After pseudouridylation assays with a saturating amount of H/ACA RNP pseudouridine synthase and nuclease P1 digestion of RNA substrates, formation of uridine (or modified uridine) isomers was detected by thin-layer chromatography. As shown in Fig. 3a, 5BrU completely inhibited isomerization.

To further provide evidence for the reactivity of 5BrU with the enzyme, we obtained a crystal structure of 5BrU in complex with the *Pyrococcus furiosus* H/ACA RNP that contains Cbf5, Nop10, L7Ae, and a guide RNA at 2.9 Å. The crystallographic data are listed in Table 1 of Supplementary Data. Its global structure bears a strong similarity to the previously determined 5FhΨ-bound RNP structure.[31,32] However, σ_A-weighted electron den-

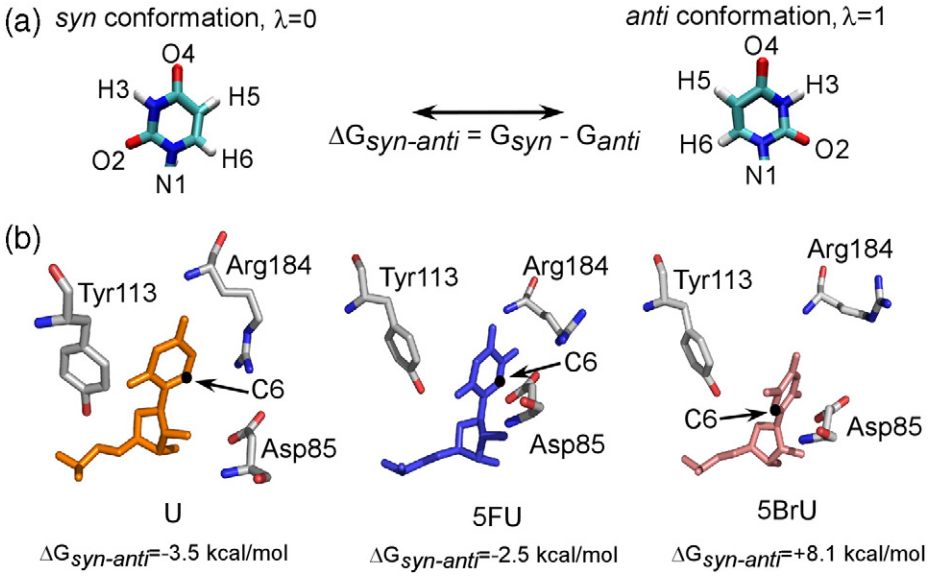

Fig. 2. Computationally identified low-energy structures of uridine (orange), 5FhΨ (blue), and 5BrU (pink). The *syn* and *anti* conformations and their free-energy difference are defined as shown in (a) and are represented by a "coupling parameter" (λ) for the calculation of free-energy difference. The computed free-energy difference after convergence is shown below each complex in (b). Details of free-energy simulation are included in Supplementary Data.

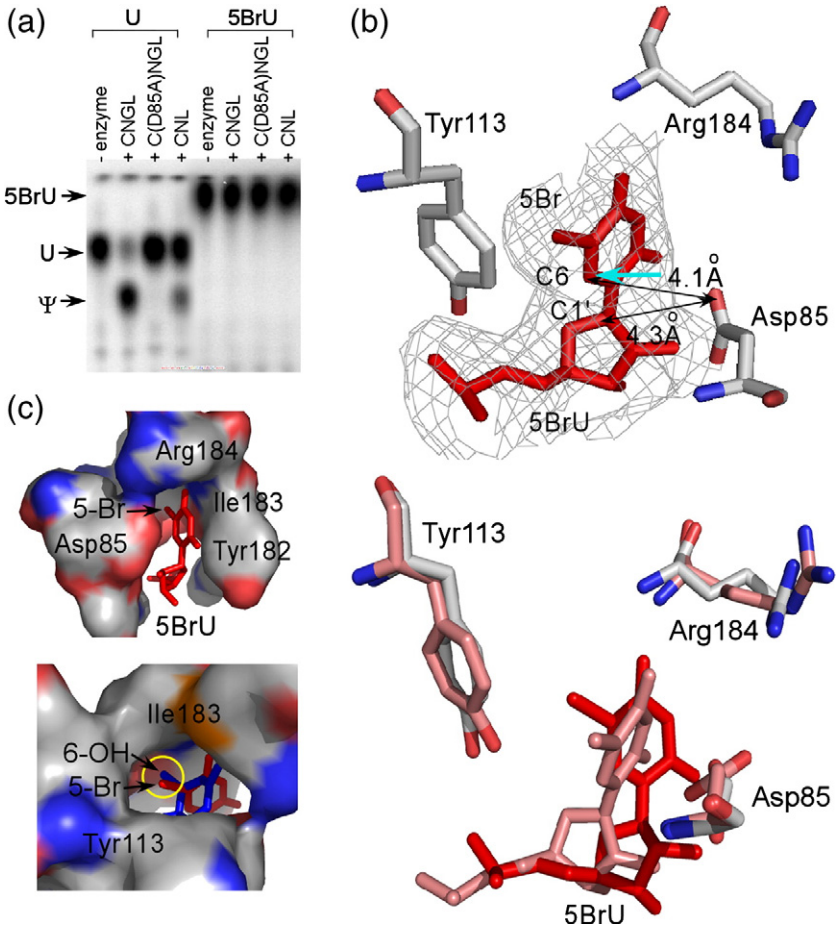

Fig. 3. Enzyme activity assay (a) and structural study results (b and c) of 5BrU bound to H/ACA RNP pseudouridine synthase. (a) Thin-layer chromatography separation of reacted and digested wild-type (U) or 5BrU substrate nucleotides. "C," Cbf5; "N," Nop10; "G," "Gar1"; "L," L7Ae. D85A is the catalytically deficient mutant of Cbf5. (b) Top: Crystal structure of the active site of the 5BrU substrate bound to H/ACA RNP. Omitted $3F_o-2F_c$ map is shown at 1.0σ around the target nucleotide. Bottom: Comparison of the computed low-energy structure (pink) to the crystal structure (red). (c) Top: 5BrU (red) is tightly bound by active-site residues (surface). Bottom: Superimposed 5FhΨ (blue) shows a similar location of the 6-hydroxyl group as 5-bromide. Experimental details for enzyme activity assay, protein crystallization, and structure determination are included in Supplementary Data.

sity maps of 5BrU clearly revealed that it did not react to the enzyme and is in the computationally predicted *anti* conformation (Fig. 3b). Although its C1′ atom has a distance to the carbonyl group of the catalytic Asp85 (4.3 Å) similar to that of 5FhΨ, its C6 atom points away from Asp85. Even though Asp85 could facilitate a nucleophilic attack on C6 in this orientation (Fig. 3b, cyan arrow), it would result in the minor *trans* 6-hydroxyl stereoisomer.[39] Therefore, 5BrU is confined to an orientation that does not permit the initial attack to take place. The bromide atom is primarily responsible for the change, since the *anti* conformation is preferred in its presence. The bromide atom is in close contact with several polar and aliphatic groups of the active site. These include the hydroxyl group of Tyr113, the amide group of Ile183, and the aliphatic group of Ile183 (Fig. 3c). Strikingly, the O6 atom in the bound 5FhΨ is located in exactly the same site and establishes similar extensive interactions with the enzyme, which likely serves to hyperstabilize the reaction intermediate (Fig. 3c).

We have demonstrated uridine's clear preference for the *syn* conformation in the microenvironment provided by the H/ACA RNP pseudouridine synthase. Perturbation of this conformation resulted in inhibition of the activity. These results highlight an important role of the pre-reactive-state glycosidic bond conformation in catalysis. Significantly, the predicted pre-reactive state conformation suggests a preference for a C6-based catalytic mechanism. Regardless of the actual mechanism of nucleophilic attack, C6-based schemes are consistent with the formation of the 5FhΨ intermediate[8,29] and the 6-hydroxyl group acquired from the aqueous solution.[8]

Accession numbers

Coordinates and structure factors have been deposited in the Protein Data Bank with accession number 3LWO.

Acknowledgements

This work was supported, in part, by National Institutes of Health grant R01 GM66958-01 (H.L.), National Science Foundation grant 0919983 (W.Y.), and American Heart Association Florida/Puerto Rico Affiliate predoctoral fellowships 0815267E (J.Z.) and 0815267E (B.L.). X-ray diffraction data were collected from the Southeast Regional Collaborative Access Team 22-ID beamline at the Advanced Photon Source, Argonne National Laboratory. Use of the Advanced Photon Source was supported by

the US Department of Energy, Office of Science, Office of Basic Energy Sciences, under contract no. W-31-109-Eng-38.

Supplementary Data

Supplementary data associated with this article can be found, in the online version, at doi:10.1016/j.jmb.2010.06.061

References

1. Charette, M. & Gray, M. W. (2000). Pseudouridine in RNA: what, where, how, and why. *IUBMB Life*, **49**, 341–351.
2. Grosjean, H. & Benne, R. (1998). *Modification and Editing of RNA.* ASM Press, Washington, DC.
3. Arnez, J. G. & Steitz, T. A. (1994). Crystal structure of unmodified tRNA(Gln) complexed with glutaminyl-tRNA synthetase and ATP suggests a possible role for pseudo-uridines in stabilization of RNA structure. *Biochemistry*, **33**, 7560–7567.
4. Newby, M. I. & Greenbaum, N. L. (2002). Investigation of Overhauser effects between pseudouridine and water protons in RNA helices. *Proc. Natl Acad. Sci. USA*, **99**, 12697–12702; Electronic publication, September 19, 2002.
5. Davis, D. R. (1995). Stabilization of RNA stacking by pseudouridine. *Nucleic Acids Res.* **23**, 5020–5026.
6. Yu, Y. T., Shu, M. D. & Steitz, J. A. (1998). Modifications of U2 snRNA are required for snRNP assembly and pre-mRNA splicing. *EMBO J.* **17**, 5783–5795.
7. King, T. H., Liu, B., McCully, R. R. & Fournier, M. J. (2003). Ribosome structure and activity are altered in cells lacking snoRNPs that form pseudouridines in the peptidyl transferase center. *Mol. Cell*, **11**, 425–435.
8. Spedaliere, C. J., Ginter, J. M., Johnston, M. V. & Mueller, E. G. (2004). The pseudouridine synthases: revisiting a mechanism that seemed settled. *J. Am. Chem. Soc.* **126**, 12758–12759.
9. Huang, L., Pookanjanatavip, M., Gu, X. & Santi, D. V. (1998). A conserved aspartate of tRNA pseudouridine synthase is essential for activity and a probable nucleophilic catalyst. *Biochemistry*, **37**, 344–351.
10. Zhao, X. & Horne, D. A. (1997). The role of cysteine residues in the rearrangement of uridine to pseudouridine catalyzed by pseudouridine synthase I. *J. Biol. Chem.* **272**, 1950–1955.
11. Sivaraman, J., Iannuzzi, P., Cygler, M. & Matte, A. (2004). Crystal structure of the RluD pseudouridine synthase catalytic module, an enzyme that modifies 23S rRNA and is essential for normal cell growth of *Escherichia coli*. *J. Mol. Biol.* **335**, 87–101.
12. Kaya, Y., Del Campo, M., Ofengand, J. & Malhotra, A. (2004). Crystal structure of TruD, a novel pseudouridine synthase with a new protein fold. *J. Biol. Chem.* **279**, 18107–18110.
13. Hoang, C. & Ferre-D'Amare, A. R. (2004). Crystal structure of the highly divergent pseudouridine synthase TruD reveals a circular permutation of a conserved fold. *RNA*, **10**, 1026–1033.
14. Sivaraman, J., Sauve, V., Larocque, R., Stura, E. A., Schrag, J. D., Cygler, M. & Matte, A. (2002). Structure of the 16S rRNA pseudouridine synthase RsuA bound to uracil and UMP. *Nat. Struct. Biol.* **9**, 353–358.
15. Dong, X., Bessho, Y., Shibata, R., Nishimoto, M., Shirouzu, M., Kuramitsu, S. & Yokoyama, S. (2006). Crystal structure of tRNA pseudouridine synthase TruA from *Thermus thermophilus* HB8. *RNA Biol.* **3**, *115–122.*
16. Del Campo, M., Ofengand, J. & Malhotra, A. (2004). Crystal structure of the catalytic domain of RluD, the only rRNA pseudouridine synthase required for normal growth of *Escherichia coli*. *RNA*, **10**, 231–239.
17. Hoang, C., Chen, J., Vizthum, C. A., Kandel, J. M., Hamilton, C. S., Mueller, E. G. & Ferre-D'Amare, A. R. (2006). Crystal structure of pseudouridine synthase RluA: indirect sequence readout through protein-induced RNA structure. *Mol. Cell*, **24**, 535–545.
18. McCleverty, C. J., Hornsby, M., Spraggon, G. & Kreusch, A. (2007). Crystal structure of human Pus10, a novel pseudouridine synthase. *J. Mol. Biol.* **373**, 1243–1254.
19. Hoang, C. & Ferre-D'Amare, A. R. (2001). Cocrystal structure of a tRNA Psi55 pseudouridine synthase: nucleotide flipping by an RNA-modifying enzyme. *Cell*, **107**, 929–939.
20. Balakin, A. G., Smith, L. & Fournier, M. J. (1996). The RNA world of the nucleolus: two major families of small RNAs defined by different box elements with related functions. *Cell*, **86**, 823–834.
21. Ganot, P., Bortolin, M. L. & Kiss, T. (1997). Site-specific pseudouridine formation in preribosomal RNA is guided by small nucleolar RNAs. *Cell*, **89**, 799–809.
22. Decatur, W. A. & Fournier, M. J. (2003). RNA-guided nucleotide modification of ribosomal and other RNAs. *J. Biol. Chem.* **278**, 695–698.
23. Baker, D. L., Youssef, O. A., Chastkofsky, M. I., Dy, D. A., Terns, R. M. & Terns, M. P. (2005). RNA-guided RNA modification: functional organization of the archaeal H/ACA RNP. *Genes Dev.* **19**, 1238–1248.
24. Meier, U. T. (2005). The many facets of H/ACA ribonucleoproteins. *Chromosoma*, **114**, 1–14.
25. Hamma, T. & Ferre-D'Amare, A. R. (2006). Pseudouridine synthases. *Chem. Biol.* **13**, 1125–1135.
26. Koonin, E. V. (1996). Pseudouridine synthases: four families of enzymes containing a putative uridine-binding motif also conserved in dUTPases and dCTP deaminases. *Nucleic Acids Res.* **24**, 2411–2415.
27. Ramamurthy, V., Swann, S. L., Paulson, J. L., Spedaliere, C. J. & Mueller, E. G. (1999). Critical aspartic acid residues in pseudouridine synthases. *J. Biol. Chem.* **274**, 22225–22230.
28. Charpentier, B., Muller, S. & Branlant, C. (2005). Reconstitution of archaeal H/ACA small ribonucleoprotein complexes active in pseudouridylation. *Nucleic Acids Res.* **33**, 3133–3144.
29. Gu, X., Liu, Y. & Santi, D. V. (1999). The mechanism of pseudouridine synthase I as deduced from its interaction with 5-fluorouracil-tRNA. *Proc. Natl Acad. Sci. USA*, **96**, 14270–14275.
30. Hamilton, C. S., Greco, T. M., Vizthum, C. A., Ginter, J. M., Johnston, M. V. & Mueller, E. G. (2006). Mechanistic investigations of the pseudouridine synthase RluA using RNA containing 5-fluorouridine. *Biochemistry*, **45**, 12029–12038.
31. Duan, J., Li, L., Lu, J., Wang, W. & Ye, K. (2009). Structural mechanism of substrate RNA recruitment in H/ACA RNA-guided pseudouridine synthase. *Mol. Cell*, **34**, 427–439.
32. Liang, B., Zhou, J., Kahen, E., Terns, R. M., Terns, M. P. & Li, H. (2009). Structure of a functional ribonucleoprotein pseudouridine synthase bound to a substrate RNA. *Nat. Struct. Mol. Biol.* **16**, 740–746.

33. Hoang, C., Hamilton, C. S., Mueller, E. G. & Ferre-D'Amare, A. R. (2005). Precursor complex structure of pseudouridine synthase TruB suggests coupling of active site perturbations to an RNA-sequestering peripheral protein domain. *Protein Sci.* **14**, 2201–2206.
34. Zheng, L. Q., Chen, M. G. & Yang, W. (2009). Simultaneous escaping of explicit and hidden free energy barriers: application of the orthogonal space random walk strategy in generalized ensemble based conformational sampling. *J. Chem. Phys.* **130**, 234105.
35. Zheng, L. Q., Chen, M. G. & Yang, W. (2008). Random walk in orthogonal space to achieve efficient free-energy simulation of complex systems. *Proc. Natl Acad. Sci. USA*, **105**, 20227–20232.
36. Tembe, B. L. & Mccammon, J. A. (1984). Ligand receptor interactions. *Comput. Chem.* **8**, *281–283.*
37. Kollman, P. (1993). Free-energy calculations—applications to chemical and biochemical phenomena. *Chem. Rev.* **93**, 2395–2417.
38. Moore, M. J. & Sharp, P. A. (1992). Site-specific modification of pre-mRNA: the 2′-hydroxyl groups at the splice sites. *Science*, **256**, 992–997.
39. Spedaliere, C. J. & Mueller, E. G. (2004). Not all pseudouridine synthases are potently inhibited by RNA containing 5-fluorouridine. *RNA*, **10**, 192–199.

Supplementary Information

Glycosidic Bond Conformation Preference Plays a Pivotal Role in Catalysis of RNA Pseudouridylation: A Combined Simulation and Structural Study

Jing Zhou[1], Chao Lv[1], Bo Liang[2], Mengen Chen[2], Wei Yang[1,2*], Hong Li[1,2,*]

[1]Department of Chemistry and Biochemistry, [2]Institute of Molecular Biophysics, Florida State University, Tallahassee, FL 32306, USA.

E-mail: hong.li@fsu.edu, yyang2@fsu.edu

METHODS

Protein expression, purification, and crystallization

Pyrococcus furiosus H/ACA RNP components were prepared as previously described[1-3]. Substrate 22mer RNA 5'-GAUGGAGCG(5BrU)GCGGUUUAAUG-3' was ordered from Dharmacon (Chicago, IL) and purified according to the manufacturer protocols. For crystallization, The full-length Pf9_Pf6 composite guide RNA[3] and 5Br-substituted substrate RNA were first mixed at a molar ratio of 1:1 and annealed by heating to 70ºC for 10 minutes and cooling down to the room temperature. Then the RNAs were combined with Cbf5, Nop10, and L7Ae at 1:1:1 molar ratio to reach the final total concentration of 20 mg/ml. The complex was then incubated at 70ºC for 30 minutes and then cooled down to 25ºC. Crystals were obtained after 3 days in 0.2M KCl, 0.15M Mg acetate, 8% PEG 6000 and 50mM cacodylate sodium pH 6.5 at 30ºC using the hanging-drop vapor diffusion method. For diffraction studies, the crystals were soaked in a cryo solution containing mother liquor plus 1.2 M KCl briefly being flash-cooled in a liquid nitrogen stream. The X-ray diffraction data were collected at Southeast Regional Collaborative Access Team (SERCAT) beamlines 22ID and 22BM beamlines at Argonne National Laboratory and were processed by HKL2000[4].

Structure Determination

The structures of box H/ACA RNP bound with 5BrU-containing substrate was solved by molecular replacement using the published coordinate for the 5FhΨ complex structure (PDB: 3HJW)[3] as the search model. A single and outstanding solution was readily identified by the program PHENIX[5] The substrate RNA was omitted in the initial

model building in order to avoid model bias. At later stages of refinement, computed $3F_o$-$2F_c$ density maps phased with proteins and the guide RNA allowed 5BrU-containing substrates to be built by COOT[6] and O[7]. The structure was refined by PHENIX[5] and the figures were prepared using the graphic program PYMOL[8]. Data collection and refinement statistics are included in Table S1.

Pseudouridylation Activity Assay

To specifically label the target nucleotide by radioisotope, we utilized the DNA splint method in which the 22mer substrates were generated by ligation of two half-oligos[9]. 5'-GGAUGGAGCG-3' and 5'-XGCGGUUUAAUG-3' where X is U and 5BrU respectively, were obtained commercially from Dharmacon (Chicago, IL) and IDT (Coralville, IA). The nucleotides X were labeled at the 5' end by using [γ-^{32}P]ATP (PerkinElmer, Waltham, MA) and T4 polynucleotide kinase reaction kit (NEB, Ipswich, MA). The 22mer substrates were then generated by using T4 DNA ligase (Invitrogen, Carlsbad, CA) and DNA template (5'-CATTAAACCGCACGCTCCATCTATAGTGAGTCGTATTAAATTC-3') (IDT, Coralville, IA). The H/ACA RNP components (protein: 3μM, guide RNA: 2.5μM) were first mixed and incubated at 70 ºC for 5 minutes in a reaction buffer containing 100mM Tris-HCl 8.0, 100 mM ammonium acetate, 5 mM $MgCl_2$, 2 mM DTT, and 0.1 mM EDTA. The labeled substrates were then added and continued incubated for additional 2 hours. After reaction, the substrates were purified by phenol extraction and ethanol precipitation as previously described[10]. Nuclease P1 (US Biological, Swampscott, MA)

was used to digest the substrates into nucleotides which were then analyzed by thin layer chromatography using solvent HCl, isopropanol and H_2O (15:70:15, v/v/v)[10].

Free energy simulations

Structure Setup

The atomic coordinates of the H/ACA RNP complex were obtained from crystal structure 3HJW. The unmodified structure and the 5-brorouridine were obtained by simple replacement of H or Br respectively. TIP3P was used as the solvent water model with octahedral box of 109Å[11]. 1000-step steepest descent minimization was performed to relax possible structural clashes in the solvated systems. The CHARMM27 force field was used for intra-molecular interactions[12].

Pseudo-Alchemical Free Energy Simulation Scheme

In order to calculate free energy difference of the inactive and active states, Orthogonal Space Random Walk (OSRW)[13,14] was used here in order to increase the efficiency of convergence. We devised a new approach based on the classical alchemical free energy perturbation scheme[15,16] to compute the free energy difference between the two conformers (the *syn* and *anti*) of the uridine base. A "coupling parameter", λ, specifies the series of non-physical intermediates for the transformation between the *syn* (λ=0) and the *anti* (λ=1) glycosidic conformations. The PERT facility in the CHARMM program[17,18] was employed to label these two states. For instance, the *anti* (λ=1) conformer of the wild-type structure can be obtained by simply varying the atom types ((H3→H5), (H5→H3), (N3→C5), (C5→N3), (C2→C6), (C6→C2), (H6→O2) and

(O2→H6)) (Fig. 2) and the corresponding atomic charges. In this manner, we fulfilled the requirement of the uridine base from one state to the other without sampling large range of conformational regions, which separate the two conformers of interest with large free energy barrier.

Simulation Setup

All the algorithms are implemented in the CHARMM program[17]. The Particle Mesh Ewald (PME) method was used to treat long-range Columbic interactions. For short-range real-space electrostatic interactions, forces are switched off starting at 8Å and totally off at 12Å. Regarding OSRW method, the height of the unit Gaussian function is 0.01 kcal/mol. The unit Gaussian widths along the two directions are 0.01 and 4.0kcal/mol, respectively. The SHAKE algorithm was applied to constrain the bonds involving hydrogen atoms. The Nose-Hoover method was employed to maintain a constant temperature at 300 K, and the Langevin piston algorithm was used to maintain the constant pressure at 1 atm. The time-step was set as 1 fs. The soft-core potential[19,20] was employed for the corresponding "alchemical" transitions. As in the original OSRW design, the λ-dynamics scheme[21,22] was utilized to couple the λ move with the physical motions.

Table S1. Data collection and refinement statistics

	5BrU
Data collection	
Space group	$P2_12_12$
Cell dimensions	
a(Å)	184.525
b(Å)	62.700
c(Å)	85.339
α, β, γ (°)	90, 90, 90
Resolution range (Å)	100.0-2.9 (3.0-2.9)
R_{sym}	0.098 (0.52)
I/σ(I)	26.7 (4.5)
Redundancy	13.4 (11.4)
Completeness (%)	99.8 (99.7)
Refinement	
Resolution Range (Å)	42.67-2.96
No. of unique reflections	21058
R_{work} / R_{free}	18.10/24.34
No. of amino-acid/nucleotide	500/71
No. of protein/RNA atoms	3882/1514
No. of waters/ions	2/1
B-factors	
Cbf5/Nop10/L7ae	82.1/93.2/131.9
guide RNA/substrate RNA	116.4/119.1
Ion/water	231.7/59.3
R.m.s deviation of the model	
Bond length (Å)	0.007
Bond angle (°)	1.240
Ramachandran plot (%)	
in most favored region	89.2
in additionally allowed region	10.3
in generously allowed region	0.5
in disallowed region	0.0

REFERENCE

1. McKenna, S. A., Kim, I., Puglisi, E. V., Lindhout, D. A., Aitken, C. E., Marshall, R. A. & Puglisi, J. D. (2007). Purification and characterization of transcribed RNAs using gel filtration chromatography. *Nat. Protoc.* **2**, 3270-7.

2. Rashid, R., Liang, B., Baker, D. L., Youssef, O. A., He, Y., Phipps, K., Terns, R. M., Terns, M. P. & Li, H. (2006). Crystal structure of a Cbf5-Nop10-Gar1 complex and implications in RNA-guided pseudouridylation and dyskeratosis congenita. *Mol. Cell* **21**, 249-60.

3. Liang, B., Zhou, J., Kahen, E., Terns, R. M., Terns, M. P. & Li, H. (2009). Structure of a functional ribonucleoprotein pseudouridine synthase bound to a substrate RNA. *Nat. Struct. Mol. Biol.* **16**, 740-6.

4. Zbyszek Otwinowski, W. M. (1997). Processing of X-ray Diffraction Data Collected in Oscillation Mode. In *Methods in Enzymology*, Vol. 276, pp. 307-326.

5. Adams, P. D., Grosse-Kunstleve, R. W., Hung, L. W., Ioerger, T. R., McCoy, A. J., Moriarty, N. W., Read, R. J., Sacchettini, J. C., Sauter, N. K. & Terwilliger, T. C. (2002). PHENIX: building new software for automated crystallographic structure determination. *Acta Crystallogr. D Biol. Crystallogr.* **58**, 1948-54.

6. Emsley, P. & Cowtan, K. (2004). Coot: model-building tools for molecular graphics. *Acta Crystallogr D Biol Crystallogr* **60**, 2126-32.

7. Jones, T. A., Zou, J. Y., Cowan, S. W. & Kjeldgaard, M. (1991). Improved methods for building protein models in electron density maps and the location of errors in these models. *Acta Crystallogr. A* **47 (Pt 2)**, 110-9.

8. Delano, W. L. (2002). The PyMOL Molecular Graphics System *http://www.pymol.org*.

9. Moore, M. J. & Sharp, P. A. (1992). Site-specific modification of pre-mRNA: the 2'-hydroxyl groups at the splice sites. *Science* **256**, 992-7.

10. Baker, D. L., Youssef, O. A., Chastkofsky, M. I., Dy, D. A., Terns, R. M. & Terns, M. P. (2005). RNA-guided RNA modification: functional organization of the archaeal H/ACA RNP. *Genes Dev.* **19**, 1238-48.

11. Jorgensen, W. L., Chandrasekhar, J., Madura, J. D., Impey, R. W. & Klein, M. L. (1983). Comparison of simple potential functions for simulating liquid water. *J. Chem. Phys.* **79**, 926-935.

12. MacKerell, A. D., Jr., B., D., Bellott, M., Dunbrack, R. L., Evanseck, J. D., Field, M. J., Fischer, S., Gao, J., Guo, H., Ha, S., Joseph-McCarthy, D., Kuchnir, L., Kuczera, K., Lau, F. T. K., Mattos, C., Michnick, S., Ngo, T., Nguyen, D. T., Prodhom, B., Reiher, W. E., Roux, B., Schlenkrich, M., Smith, J. C., Stote, R., Straub, J., Watanabe, M., Wirkiewicz-Kuczera, J., Yin, D. & Karplus, M. J. (1998). All-Atom Empirical Potential for Molecular Modeling and Dynamics Studies of Proteins. *J. Phys. Chem. B* **102** 3586–3616.

13. Zheng, L. Q., Chen, M. G. & Yang, W. (2009). Simultaneous escaping of explicit and hidden free energy barriers: Application of the orthogonal space random walk strategy in generalized ensemble based conformational sampling. *J. Chem. Phys.* **130**, -.

14. Zheng, L. Q., Chen, M. G. & Yang, W. (2008). Random walk in orthogonal space to achieve efficient free-energy simulation of complex systems. *Proc. Natl. Acad. Sci. USA* **105**, 20227-20232.

15. Kollman, P. (1993). Free-Energy Calculations - Applications to Chemical and Biochemical Phenomena. *Chemical Reviews* **93**, 2395-2417.

16. Tembe, B. L. & Mccammon, J. A. (1984). Ligand Receptor Interactions. *Computers & Chemistry* **8**, 281-283.

17. Brooks, B. R., Bruccoleri, R. E., Olafson, B. D., States|, D. J., Swaminathan, S. & Karplus, M. (1983). CHARMM: A program for macromolecular energy, minimization, and dynamics calculations. *J. Comp. Chem.* **4**, 187 - 217.

18. Brooks, B. R., Brooks, C. L., 3rd, Mackerell, A. D., Jr., Nilsson, L., Petrella, R. J., Roux, B., Won, Y., Archontis, G., Bartels, C., Boresch, S., Caflisch, A., Caves, L., Cui, Q., Dinner, A. R., Feig, M., Fischer, S., Gao, J., Hodoscek, M., Im, W., Kuczera, K., Lazaridis, T., Ma, J., Ovchinnikov, V., Paci, E., Pastor, R. W., Post, C. B., Pu, J. Z., Schaefer, M., Tidor, B., Venable, R. M., Woodcock, H. L., Wu, X., Yang, W., York, D. M. & Karplus, M. (2009). CHARMM: the biomolecular simulation program. *J. Comp. Chem.* **30**, 1545-614.

19. Zacharias, M., Straatsma, T. P. & Mccammon, J. A. (1994). Separation-Shifted Scaling, a New Scaling Method for Lennard-Jones Interactions in Thermodynamic Integration. *J. Chem. Phys.* **100**, 9025-9031.

20. Steinbrecher, T., Mobley, D. L. & Case, D. A. (2007). Nonlinear scaling schemes for Lennard-Jones interactions in free energy calculations. *J. Chem. Phys.* **127**, -.

21. Kong, X. J. & Brooks, C. L. (1996). lambda-Dynamics: A new approach to free energy calculations. *J. Chem. Phys.* **105**, 2414-2423.

22. Knight, J. L. & Brooks, C. L. (2009). lambda-Dynamics Free Energy Simulation Methods. *J. Comp. Chem.* **30**, 1692-1700.